Available online at www.sciencedirect.com
SCIENCE DIRECT®
ELSEVIER
International Journal of Mechanical Sciences 45 (2003) 1391–1410
International Journal of MECHANICAL SCIENCES
www.elsevier.com/locate/ijmecsci

Analysis of engine vibration and design of an applicable diagnosing approach

Zunmin Geng[a,*], Jin Chen[a], J. Barry Hull[b]

[a] *State Key Lab on Vibration, Shock & Noise, Shanghai Jiao Tong University, Shanghai 200030, People's Republic of China*

[b] *School of Engineering, The Nottingham Trent University, Burton Street, Nottingham NG1 4BU, UK*

Received 10 August 2001; received in revised form 20 September 2003; accepted 27 September 2003

Abstract

Impact excitations, time-varying transfer properties and non-stationary random response are typical characteristics of the reciprocating engine vibration. These characteristics of the engine vibration make its dynamic analysis and signature extraction much more difficult than that of the rotational machinery. Focused on this problem, this paper summarizes a thorough investigation into it from theoretical analysis to an applicable diagnosing approach design, as well as experimental verification. Firstly, the impact excitations inside the engine are reasonably analyzed and classified. Based upon this, an analytic model of the non-stationary engine vibration considering its time-varying transfer properties is developed and discussed in details on its time domain and time-frequency domain characteristics. Directed by these discussions, an applicable signature extracting and diagnosing approach is designed. This includes the software-based synchronization for pretreatment of the non-stationary vibration signal, wavelet packet based multi-band filtering techniques for signature extraction of the impact excitations, as well as the auto-regressive model based pseudo-Wigner-Ville distribution for an integrated time-frequency signature extraction of the engine vibration. These methodologies are successfully used in the practical diagnosis of the 6190Z_LC diesel engine.

Keywords: Non-stationary vibration; Machine condition monitoring; Reciprocating engine

1. Introduction

It is well known that the traditional periodogram-based vibration analysis and signature extraction is an effective approach for the dynamic analysis and fault diagnosis of the rotational machinery.

* Corresponding author. 74A Dennis Avenue, Beeston, Nottingham NG9 2PR, UK. Tel.: +44-0115-9257137; fax: +44-0161-2004646.

E-mail address: zunmin.geng@ntu.ac.uk (Z. Geng).

0020-7403/$ - see front matter © 2003 Elsevier Ltd. All rights reserved.
doi:10.1016/j.ijmecsci.2003.09.012

Nomenclature

$a_r(n)$	Gaussian-distributed white noise
C	wave celerity of the inner-cylinder gas oscillation
D	diameter of the engine cylinder
D_b	diameter of the bearing's rolling elements.
D_f	diameter of the cavitation bubbles.
$D_{uf}(r_i,t)$	mean square deviation of the vibration response $u_f(r_i,t)$
E_b	elasticity modulus of the bearing
$E(V_n^2)$	mean square deviation of V_n
$f_0(T_0)$	fundamental frequency (time-period) in a crankshaft revolution
f_1	oscillating frequency of the computer
f_2	synchronizing frequency in a crankshaft revolution
$f_s = N_s f_0$	sampling frequency in a synchronized crankshaft revolution
$f_c(r_i,t)$	stationary component of the inner-cylinder excitation $f(r_i,t)$
$f_n(r_i,t)$	Gaussian component of $f(r_i,t)$
f_b	resonant frequency of the ball elements in the bearing
G, H	orthogonal conjugate high-pass differential filter and low-pass average filter of the wavelet-packet.
$h(r_i,t)$	generalized time-varying transfer routes of the engine vibration
$H(r_i,\omega), H(r_i,t,\omega)$	stationary and time-varying Fourier Transforms of $h(r_i,t)$
$H^*(r_i,\omega), H^*(r_i,t,\omega)$	conjugates of $H(r_i,\omega)$ and $H(r_i,t,\omega)$
$m_{uf}, m_{uv}, m_{Vn}, m_w, m_{wfn}$	mean-values of $u_f(r_i,t)$, $u_v(r_i,t)$, V_n, $w(r_j,\tau_n)$ and $f_n(r_i,t)$
$M_s = f_1/f_s = f_2/f_0$	final sampling frequency ratio
N_s	sampling number in a crankshaft revolution
$N(r_j,t)$	counting variable of the Poisson process
$n(t)$	random noise with Gaussian distribution
P	indicating power expression of the diesel engine
P_f	breaking pressure of the cavitation bubbles
P_T	probability density functions of $\Phi_T(n)$
P_R	probability density functions of $\Phi_R(n)$
p	the inner-cylinder gas pressure
r and φ	parameters (radius and angle) of the polar coordinate
R	radius of the ball elements
$R_u(t_1,t_2)$	stationary auto-correlation function of the non-stationary vibration $u(t)$
$R_{uf}(r_i,t,\tau)$, $R_{uv}(r_j,t,\tau)$, $R_w(r_j,t,\tau)$, $R_\lambda(r_j,t,\tau)$	time-varying auto-correlation function of $u_f(r_i,t)$, $u_v(r_j,t)$, $w(r_j,\tau_n)$ and $\lambda(r_j,t)$
r_i	generalized transfer distance to the vibration sensor
$r_u(n,k)$	time-varying variable of PWVD
$r_{ua}(n,k)$	analytic transform of $r_u(n,k)$
$S_f(r_i,\omega), S_{fn}(r_i,\omega)$	power spectrum of $f(r_i,t)$ and $f_n(r_i,t)$
$S_{uf}(r_i,\omega_1,\omega_2), S_f(r_i,\omega_1,\omega_2)$	bi-spectrum of $u_f(r_i,t)$ and $f(r_i,t)$

$u(t)$	non-stationary vibration response of the reciprocating engine
V_n	impact intensity of the Poisson process, $n = 1, 2, \ldots, N(r_j, t)$
$v(r_j, t)$	impact-induced random vibration response
$W_{uf}(r_i, t, \omega)$, $W_f(r_i, t, \omega)$, $W_{uv}(r_i, t, \omega)$, $W_w(r_i, t, \omega)$, $W_\lambda(r_i, t, \omega)$	continuous Wigner-Ville transform of $u_f(r_i, t)$, $f(r_i, t)$, $u_v(r_i, t)$, $w(r_j, \tau_n)$ and $\lambda(r_j, t)$
$W_u^C(n, \omega)$	Clessen definition based PWVD of $u(n)$
$W_u^P(n, \omega)$	Peyrin definition based PWVD of $u(n)$
$W_u^{AR}(n, \omega)$	AR-PWVD of $u(n)$
$\underset{t}{*}$	convolution along the time axis
$w(r_j, \tau_n)$	impact waveform of the Poisson process, $n = 1, 2, \ldots, N(r_j, t)$
ω	angular frequency
$\sigma_{ar}^2(n)$	residual error of the Gaussian-distributed white noise $a_r(n)$
γ	eigenvalue of the standing-wave equation (1).
$\gamma_{n,j}$	the jth eigenvalue corresponding to m solutions of the n order Bessel equation (2) ($j = 1, \ldots, m$)
$\gamma_{R \text{ or } T}(n)$	auto-correlation matrix of the time-varying variable $r_{ua}(n, k)$
ρ_b	material density of the ball bearing
ρ_f	fluid density
τ_n	impact happening time of the Poisson process, $n = 1, 2, \ldots, N(r_j, t)$
$\varphi_r(n, i)$	auto-regressive coefficient of the M order AR (n, M) model

However, until recently, few publications have shown successful applications of this approach to the reciprocating engine, although many efforts have been made to it world widely [1–6]. Practical achievement in this area seems to be more difficult than commonly anticipated in spite of its important significance both in academia and industry.

Previous work [3–6] has highlighted the important influences of impact excitations, time-varying transfer properties and non-stationary random response in engine vibration. Consequently, these make the measured engine casing vibration signal so complex that no significant signature can be directly extracted from its frequency spectrum. As a preliminary investigation focused on the rigorous signature extraction of the inner-engine dynamic process and an applicable design of corresponding diagnostic strategies, this paper details a thorough investigation into it from theoretical deduction to applicable approach design, as well as experimental verification. The validity of these approaches is verified by comparison with experimental results from the 6190Z_LC diesel engine.

2. Impact excitations inside the engine

A basic correlation amongst the inner-cylinder combustion pressure, indicting power expression and surface vibration of the 6190Z_LC diesel engine (Jinan engine Ltd., China. Mainly for marine use, 4 strokes, 6 cylinders vertically, cylinder diameters: 190 mm, maximum speed: 3000 rev/min) is

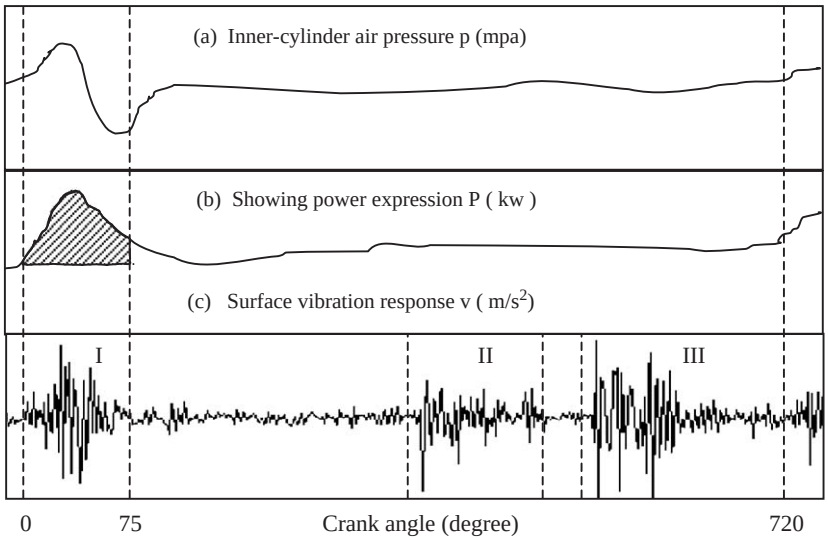

Fig. 1. Basic dynamical correlation in a diesel engine: (a) by 5 Hz high-pass filtering, (b) shadow region: the effective power and (c) impact segments from: I-Combustion excitation, II-Outlet valve, III-Inlet valve.

shown in Fig. 1 [2–4]. Actually, it expresses a mutually dependent connection amongst the inner-cylinder working process, relative transmission relationship of the mechanical systems and the dynamic performance of the engine. Obviously, the inner-cylinder working process dominates the dynamic performance of the engine and results in the largest and most significant impact excitation in it (the combustion impact). At the same time, the widespread mechanical and fluid impacts inside the engine form its high-frequency excitations. It is necessary to make an in-depth discussion to them and their influences to the engine vibration response.

2.1. The unstable combustion excitation

As derived in Ref. [3], the inner-cylinder high-pressure gas oscillation (segment I in Fig. 1) inside a diesel engine can be theoretically describe as a standing-wave equation in polar coordinates as follows:

$$\frac{1}{r}\frac{\partial}{\partial r}\left(r\frac{\partial p}{\partial r}\right)+\frac{1}{r^2}\frac{\partial^2 p}{\partial \varphi^2}+\gamma^2 p=0. \tag{1}$$

Taking the cylinder as a rigid constraint to the inner-cylinder gas oscillation, the boundary condition of Eq. (1) around the cylinder diameter D can be supposed as: $\frac{\partial p}{\partial r}|_{r=D/2}=0$.

Supposing its generalized solution as $p(r,\varphi)=\sum_{n=1}^{\infty} p_n\cos(n\varphi+\alpha_n)$, then Eq. (1) can be rewritten as:

$$\frac{\mathrm{d}^2 p_n}{\mathrm{d}r^2}+\frac{1}{r}\frac{\mathrm{d}p_n}{\mathrm{d}r}+\left(\gamma^2-\frac{n^2}{r^2}\right)p_n=0 \tag{2}$$

Eq. (2) is a typical Bessel equation [7,8]. By Laplace transformation it is possible to show that

$$p_n = J_n(k_p r), \quad p(r,\varphi) = \sum_{n=1}^{\infty} J_n(k_p r)\cos(n\varphi + \alpha_n). \tag{3}$$

Introducing the above-mentioned boundary condition into Eq. (3) to confirm the eigenvalue γ, the frequency composition of the inner-cylinder gas oscillation can be expressed as

$$f_j = \frac{1}{\pi}\frac{C}{D}\gamma_{n,j}, \quad (j = 1,2,\ldots,m). \tag{4}$$

In a theoretical sense, Eq. (4) expresses a definite description on the inner-cylinder gas oscillation. Firstly, m kinds of solution of the n order Bessel equation (2) explain the existence of unstable inner-cylinder gas oscillation with m kinds of frequency composition (single or complex). Secondly, it is shown that the actual oscillating waveform and frequency composition are mainly influenced by the structural and/or working conditions of the engine, such as the geometrical parameters of the cylinder (dimension and clearance, etc.), the inner-cylinder oil and gas pressure and their mixing and combustion status etc. This explains that the inner-cylinder gas pressure with an unstable frequency composition is a major cause of the unstable working performance and non-stationary dynamic process of the engine, and it is also directly related to the structural and working conditions of the engine.

2.2. The modulated high-frequency excitations

In Fig. 1, there is also some high frequency impulses (segments II and III) modulated by the relative transmission relationship of the sub-mechanical systems in the engine. These high frequency impulses can be classified into two groups:

2.2.1. Fluid impact induced noise

Fluid impacts are important sources of the high-frequency vibration and noise inside the engine. Taking the often-encountered cavitation noise for example, its spectrum has a wide-band distribution with a maximum frequency equal to (shown in Fig. 2) [1]

$$f = (1/2D_f)\sqrt{P_f/\rho_f} \quad \text{(Hz)}. \tag{5}$$

More generally, Lyon [2] theoretically and experimentally explained the mechanism of the fluid impact induced high-frequency noise and, based up on this, Geng [3] proved that the fluid impact induced high-frequency noise in the reciprocating engine possesses a permanent frequency composition which does not vary with changes of the engine operating condition.

2.2.2. Mechanical impacts

The widely existing transient impacts caused by the inner-engine mechanical systems tend to be periodic at the operating rate of the engine when they cause high-frequency resonant responses of the impacting mechanical parts. Examples of this are the impacts caused by the inlet and outlet valves (shown in Fig. 1: segments II and III, also discussed in details in Ref. [2]) as well as the fatigue eroding of ball bearings, etc. The high-frequency resonant response possesses permanent frequency compositions and successively transforms itself as one part of the engine vibration.

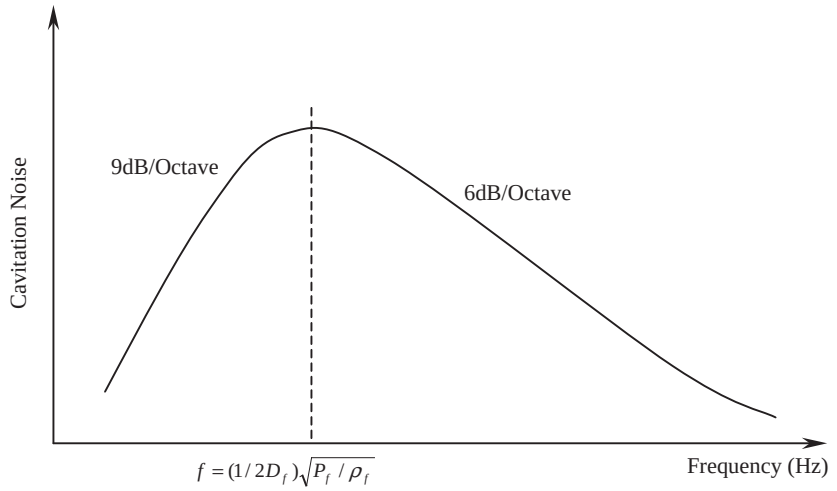

Fig. 2. Fluid impact induced high-frequency noise.

Fig. 3 shows a successful diagnosing result of the ball bearing fatigue eroding impact, from the timing system of 6190Z_LC diesel engine. This result is obtained by applying the high-frequency vibro-acoustic sensoring and high-pass filtering techniques [4]. Its maximum frequency component accords with the resonant frequency of the ball elements in the bearing and hence verifies the above description [1]

$$f = (0.848/D_b)\sqrt{E_b/2\rho_b} \quad \text{(Hz)}. \tag{6}$$

In summary, the transient response caused by the inner-engine mechanical and fluid impacts possesses permanent frequency compositions. At the same time, the unstable inner-cylinder working process and relative transmission relationship of the inner-engine mechanical systems irregularly modulate them. In consequence, the practically measured vibration signal on the engine casing expresses as a series of impulses modulated along the time history. Academically, this kind of time-varying impulsive signal can be classified as a specific type of point process, which is frequently encountered in the biomedical signal processing [1,2]. Based upon the definition of point process, each impulse can be distinguished from the others by its impact intensity V_n (location and manner of the impacts) and occurrence time τ_n (relative transmission relationship of the inner-engine mechanical systems). Considering the irregularity of the engine combustion process as well as the randomicity of the impact occurrence, the impact counting variable $N(r_j, t)$ is taken into account. Also considering the different type of impacts, respectively, caused by mechanical or fluid impact, the waveform of every impact arrived at time τ_n is introduced, denoted as $w(r_j, \tau_n)$. Then a global expression of the impact vibration response can be generally expressed as

$$v(r_j, t) = \sum_{n=1}^{N(r_j,t)} V_n\, w(r_j, \tau_n) = \sum_{n=1}^{N(r_j,t)} V_n\, w(r_j, t) \times \delta(t - \tau_n). \tag{7}$$

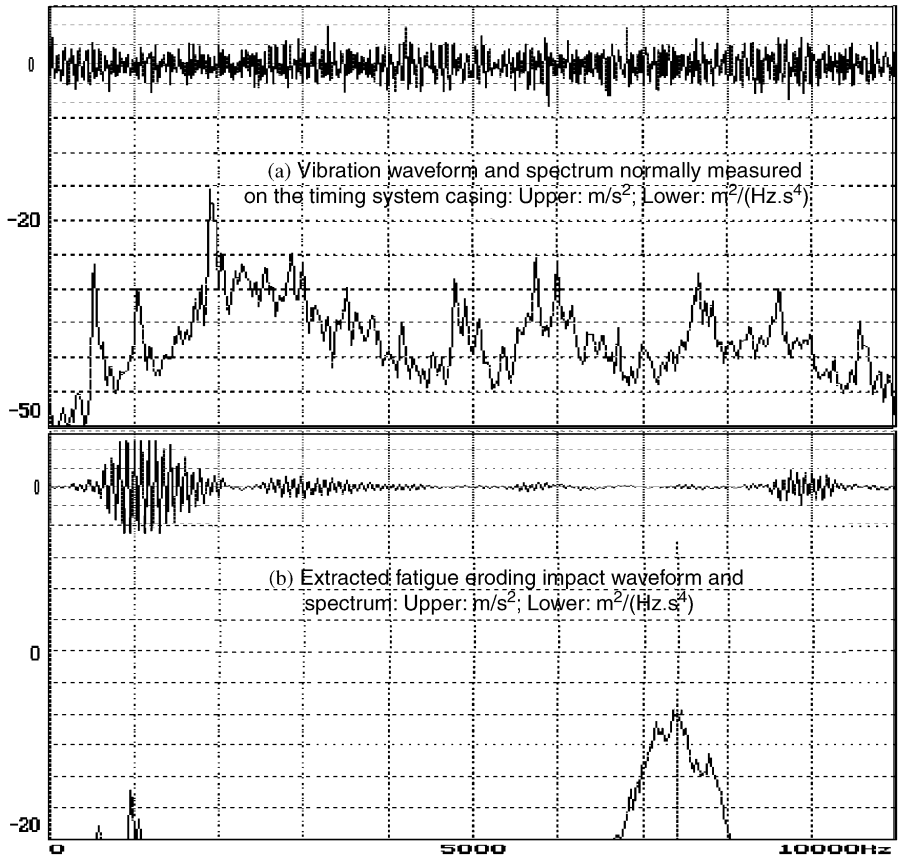

Fig. 3. The fatigue eroding impacts in a ball bearing.

3. Random vibration response of the engine

Based on the above discussions and considering the time-varying transfer routes $h(r_i,t)$ from the inner-engine excitations $f(r_i,t)$ $(i=1,2,\ldots,m)$, as well as the influences of inner-engine vibro-impact $v(r_j,t)$ $(j=1,2,\ldots,l)$, to its global surface vibration response, the non-stationary vibration response of the reciprocating engine can be expressed as

$$u(t)=\sum_{i=1}^{m}u_f(r_i,t)+\sum_{j=1}^{l}u_v(r_j,t)+n(t)$$

$$=\sum_{i=1}^{m}\int_0^t h(r_i,t-\tau)\,f(r_i,\tau)\,\mathrm{d}\tau+\sum_{j=1}^{l}v(r_j,t)+n(t). \tag{8}$$

Eq. (8) describes the overall vibration response of an engine. $u_f(r_i,t)$ presents a major component of it, caused by the inner-cylinder working process, which dominates the non-stationary vibration property of the whole engine; while the component $u_v(r_j,t)$ is mainly caused by the mechanical and

fluid impact, acts as a typical time-varying point process and contributes to the overall vibration response. Further derivation of Eq. (8) is essential for an in-depth understanding of the engine vibration.

3.1. Time-domain analysis

3.1.1. The non-stationary response $u_f(r_i,t)$

According to Eq. (4), as a general expression, $f(r_i,t)$ can be set as a product of a stationary component $f_c(r_i,t)$ with a Gaussian random component $f_n(r_i,t)$: $f(r_i,t) = f_c(r_i,t)\ f_n(r_i,t)$. Then the mean-value of the vibration response $u_f(r_i,t)$ can be derived as

$$m_{uf}(r_i,t) = m_{fn}\int_0^t h(r_i,t-\tau)\, f_c(r_i,\tau)\,\mathrm{d}\tau. \tag{9}$$

Its time-varying auto-correlation function can be derived as

$$\begin{aligned} R_{uf}(r_i,t,\tau) &= \int_0^{t+\tau/2}\int_0^{t-\tau/2} h\left(r_i,t+\frac{\tau}{2}-t_1\right)\, h\left(r_i,t-\frac{\tau}{2}-t_2\right)\, f(r_i,t_1)\, f(r_i,t_2)\,\mathrm{d}t_1\,\mathrm{d}t_2 \\ &= \int_{-\infty}^{\infty} S_{fn}(r_i,\omega)\, I\left(r_i,t+\frac{\tau}{2},\omega\right) I^*\left(r_i,t-\frac{\tau}{2},\omega\right)\,\mathrm{d}\omega, \end{aligned} \tag{10}$$

where $I(r_i,t,\omega) = \int_0^t h(r_i,t-\tau)\, f_c(r_i,\tau)\, \mathrm{e}^{\mathrm{j}\omega r}\,\mathrm{d}\tau$.

Setting $\tau = 0$, then the mean square function of $u_f(r_i,t)$ is

$$D_{uf}(r_i,t) = \int_{-\infty}^{\infty} S_{fn}(r_i,\omega)\,|I(r_i,t,\omega)|^2\,\mathrm{d}\omega. \tag{11}$$

The above derivations clearly demonstrate the co-modulating effect of $f(r_i,t)$ and $h(r_i,t)$ on the non-stationary vibration $u_f(r_i,t)$. Firstly, the time-varying mean-value shown in Eq. (9) and frequency-dependant mean-square function shown in Eq. (11) explains the difficulty in recovering the time-domain excitation waveform $f(r_i,t)$ by ordinary stationary signal processing methods, as are currently attempted by some researchers [2,7]. Secondly, as shown in Eqs. (10) and (11), high-order frequency or time-frequency expression is essential, even for the time-domain description of this kind of time-varying signal, so does the high-order frequency or time-frequency signal processing methods (refer to our practical method design in Section 4). Finally, Eqs. (9)–(11) also indicates that effective elimination of the Gaussian random component $f_n(r_i,t)$ is an important factor in the statistical signature extraction of the excitation sources (also refer to our practical method design in Section 4).

3.1.2. The time-varying Poisson process $u_v(r_j,t)$

Describing the statistic characteristics of the Poisson process $u_v(r_j,t)$, its mean-value may begin with

$$m_{uv}(r_j,t) = m_{V_n}\, m_w(r_j,t)\,\lambda(r_j,t). \tag{12}$$

Its time-varying auto-correlation function as

$$R_{uv}(r_j,t,\tau)=\int_0^t u_v\left(r_j,t+\frac{\tau}{2}\right)\,u_v\left(r_j,t-\frac{\tau}{2}\right)\,\mathrm{d}t=E(V_n^2)\,R_w(r_j,t,\tau)\,R_\lambda(r_j,t,\tau), \tag{13}$$

where $\lambda(r_j,t)=E[\mathrm{d}N(r_j,t)/\mathrm{d}t]$.

Eqs. (12) and (13) clearly indicate that the statistical parameters of the time-varying Poisson process $u_v(r_j,t)$ are sensitive to the impact intensity V_n as well as the non-stationary working process of the engine. It suggests that a well-designed time-varying statistical approach will be effective in extracting the time-domain signatures of the high-frequency mechanical and fluid impacts (refer to our practical method design in Section 4).

3.2. Frequency domain analysis

As naturally derived from Eqs. (10) and (11), the high-order time-frequency expression $I(r_i,t,\omega)$ (under certain conditions, it can be transferred into a high-order frequency expression) is introduced into the time-varying vibration description. This means, high-order frequency or time-frequency analysis is essential in this research. As a well-defined and widely recognized means for high-order frequency analysis, the Bi-spectrum is traditionally used both for theoretic analytics and experimental signal analysis [9,10]. From another point, the more advanced Wigner-Ville time-frequency distribution supplies a powerful tool for time-frequency analysis [11–13]. In order to compare between both the two approaches and reach a reasonable solution for the engine vibration analysis, the following derivations and discussions are made to the high-order frequency and time-frequency characteristics of the engine vibration.

3.2.1. Bi-spectral analysis

Theoretically, the Bi-spectral expression of the non-stationary vibration $u(t)$ is based upon a stationary correlation definition [9,10]

$$\begin{aligned}R_u(t_1,t_2)&=\int_0^{t_1}\int_0^{t_2}u(t)\,u(\tau)\,\mathrm{d}t\,\mathrm{d}\tau\\&=R_u(t_1,\tau)=\int_0^{t_1}u(t)\,u(t+\tau)\,\mathrm{d}t=R_u(t_1,-\tau)=\int_0^{t_1}u(t)\,u(t-\tau)\,\mathrm{d}t.\end{aligned} \tag{14}$$

Based on this definition, the Bi-spectrum of $u_f(r_i,t)$ can be further derived as

$$\begin{aligned}S_{uf}(r_i,\omega_1,\omega_2)&=\int_{-\infty}^{\infty}\int_{-\infty}^{\infty}u_f(r_i,t_1)\,u_f(r_i,t_2)\mathrm{e}^{-\mathrm{j}(\omega_1t_1-\omega_2t_2)}\,\mathrm{d}t_1\,\mathrm{d}t_2\\&=H(r_i,t_1,\omega_1)\,H^*(r_i,t_2,\omega_2)\,S_f(r_i,\omega_1,\omega_2).\end{aligned} \tag{15.1}$$

When the transfer function $h(r_i,t)$ is stationary and the excitation $f(r_i,t)$ is non-stationary, Eq. (15.1) can be simplified as

$$S_{uf}(r_i,\omega_1,\omega_2)=H(r_i,\omega_1)\,H^*(r_i,\omega_2)\,S_f(r_i,\omega_1,\omega_2). \tag{15.2}$$

When the transfer function $h(r_i,t)$ is time-varying and the excitation $f(r_i,t)$ is stationary, it can be further simplified as

$$S_{uf}(r_i,\omega_1,\omega_2)=H(r_i,t_1,\omega_1)\,H^*(r_i,t_2,\omega_2)\,S_f(r_i,\omega_1,\omega_2)\delta(\omega_2-\omega_1). \tag{15.3}$$

When both the transfer function $h(r_i,t)$ and the excitation $f(r_i,t)$ are stationary, it returns to the traditional spectral expression for a stationary random vibration

$$S_{uf}(r_i,\omega) = |H(r_i,\omega)|^2 S_f(r_i,\omega). \tag{15.4}$$

With the same definition, the Bi-spectrum of $u_v(r_j,t)$ can be derived as:

$$S_{uv}(r_j,\omega_1,\omega_2) = 2\pi E[V_n^2] S_w(r_j,t_1,\omega_1) S_w^*(r_j,t_2,\omega_2) S_\lambda(r_j,\omega_1-\omega_2). \tag{16}$$

With the Bi-spectrum definition, Eq. (15) presents a combined reflection, respectively, from the conjugate time-varying transfer route $H(r_i,t_1,\omega_1)$, $H^*(r_i,t_2,\omega_2)$, as well as the high-order spectrum of excitation $S_f(r_i,\omega_1,\omega_2)$ (same to Eq. (16)). This means, its physical explanation for the engine vibration will be confusing and very hard to understand. A simple example is as shown in Eq. (15.3), its description for a stationary transfer function coupled with a non-stationary excitation is often the same as for a time-varying transfer function coupled with a stationary excitation, so as to confuse the time-varying characteristics of the engine vibration. Another vital disadvantage of Bi-spectrum in describing the time-varying engine vibration can be directly found from the even-symmetry assumption of its stationary correlation $R_u(t_1,\tau) = R_u(t_1,-\tau)$ as shown in Eq. (14), which ensures the non-negative real values of the Bi-spectrum [9]. Actually, when the engine vibration response $u(t)$ is non-stationary, $R_u(t_1,\tau) \neq R_u(t_1,-\tau)$. This non-even-symmetry characteristics of its stationary correlation means that the Bi-spectral expression may not only comprise of real-values, therefore its physical explanation for the engine vibration might be unreasonable.

3.2.2. *Time-frequency spectral analysis*

Contrasting to Eq. (14), a more reasonable non-stationary correlation definition as shown in Eqs. (10) and (13) is introduced into the time-frequency expression of engine vibration [11,12]. This definition ensures the even-symmetry of the non-stationary correlation, i.e. $R_u(t,t+\tau) = R_u(t,t-\tau) = R_u(t+(\tau/2),t-(\tau/2))$. Same to the above-mentioned Bi-spectrum, its time-frequency characteristics are derived as follows.

For the non-stationary response $u_f(r_i,t)$, its time-frequency spectrum expression can be derived as

$$W_{uf}(r_i,t,\omega) = \int_{-\infty}^{\infty} u_f\left(r_i,t+\frac{\tau}{2}\right) u_f\left(r_i,t-\frac{\tau}{2}\right) \mathrm{e}^{-\mathrm{j}\omega\tau}\,\mathrm{d}\tau = H(r_i,t,\omega) \underset{t}{*} W_f(r_i,t,\omega). \tag{17}$$

For the Poisson process $u_v(r_j,t)$, its time-frequency spectrum can be derived as

$$W_{uv}(r_j,t,\omega) = E(V_k^2)\, W_w(r_j,t,\omega) \underset{t}{*} W_\lambda(r_j,t,\omega). \tag{18}$$

These time-frequency expressions for the engine vibration show some special advantages over its Bi-spectral expression. Firstly, the even-symmetry of its non-stationary correlation guarantees real values in its time-frequency expressions and therefore allows a definite physical explanation. Secondly, descriptions of the vibration compositions are expressed as convolutions of the time-varying transfer function with non-stationary excitations along the time axis. This feature possesses special significance for the time-frequency signature extraction of the excitations (refer to our practical method design in Section 4).

4. Applicable diagnosing approach design

Directed by the above-mentioned theoretical analysis, an applicable diagnosing approach is designed and successfully applied to the 6190Z_LC diesel engine. All the experimental results coincided perfectly with the theoretical derivations and therefore verified the validity and practicability of this approach.

4.1. Software-based synchronizing filtering

In order to effectively eliminate the time-varying random noise as discussed in Eqs. (9)–(11), also get a clarified Poisson process $u_v(r_j,t)$ discussed in Eq. (13), a software-based instantaneous synchronizing filter is designed for pre-treatment of the engine vibration signal in Fig. 4 [3,4].

Compared with the traditional phase-locked loop (PLL) technique [1,2], this method exactly delays one crankshaft revolution to instantaneously lock the sampling phase and period. Although there is always a sampling error between $M_s \leqslant T_0 f_2 < M_s + 1$, its influence on the filtering accuracy can be neglected because of the high oscillating frequency of the computer f_1. At the same time, the Poisson process counting variable $N(r_j,t)$ can also be obtained easily. A comparison of unfiltered and filtered vibration signals measured from the 6190Z_LC diesel engine casing is provided in Fig. 5.

4.2. Excitation signatures' extraction

As outlined in Eqs. (4) and (7), different kinds of excitation inside the engine presents different impact signatures, further modulated by the time-varying transfer properties of the reciprocating engine. Therefore, specially designed multi-band pass and/or resistant filtering techniques are essential for these signature extractions. In this paper, a successful application of this strategy is the wavelet packet based multi-band synchronizing optimal filtering technique [4].

4.2.1. Decomposition algorithm of the wavelet-packet [12,13]

According to the wavelet algorithm [14,15], the time-varying engine vibration signal $u(t)$ can be further represented as its wavelet decomposition form

$$u(t) = A_{J_2}u(t) + \sum_{j=J_1}^{J_2} D_j u(t) = \sum_{k\in Z} C_{J_2k}\varphi_{J_2k}(t) + \sum_{j=J_1+1,k\in Z}^{J_2} \psi_{jk}(t), \tag{19}$$

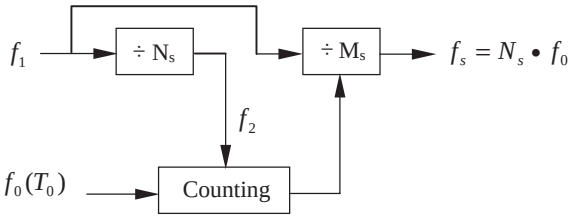

Fig. 4. Software-based instantaneous synchronizing filter.

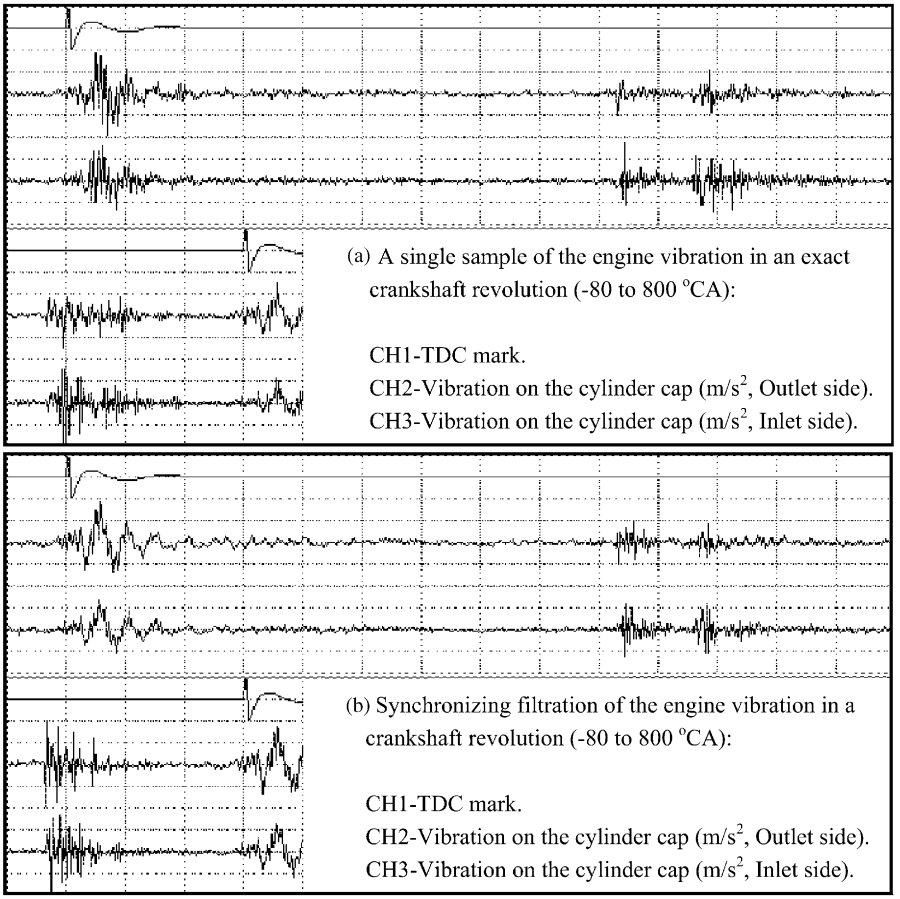

Fig. 5. Instantaneously synchronizing filtration of the engine vibration.

where $A_{J_2}u(t)=\sum_{k\in Z} C_{J_2k}\varphi_{J_2k}(t)$ represents the signal components which frequencies are lower than 2^{-J_2}, whilst $D_ju(t)=\sum_{k\in Z}\psi_{jk}(t)$ represents the signal components which frequencies are between 2^{-j} and $2^{-(j-1)}$. Sampling point $j=J_1,\ldots,J_2-1$.

Further representing Eq. (19) into the combination form of its low-pass Average-Filter H and high-pass Differential-Filter G, it can be expressed as follows:

$$C_{j+1}=HC_j;\quad D_{j+1}=GC_j;\quad j=J_1,\ldots,J_2-1. \tag{20}$$

Referring to the commonly accepted approaches [14,15], decomposition algorithm of the wavelet-packet proceeds with its two-to-one sampling by a serial of orthogonal conjugate filters H and G. Supposing $C_{i,j}$ as its ith by jth scale factor, then

$$C_{1,0}(t)=u(t);\quad C_{2i-1,j}(t)=HC_{i,j-1}(t);\quad C_{2i,j}(t)=GC_{i,j-1}(t)$$
$$t=1,\ldots,2^{J-j};\quad i=1,\ldots,2^j;\quad j=1,\ldots,J;\quad J=\log_2 N. \tag{21}$$

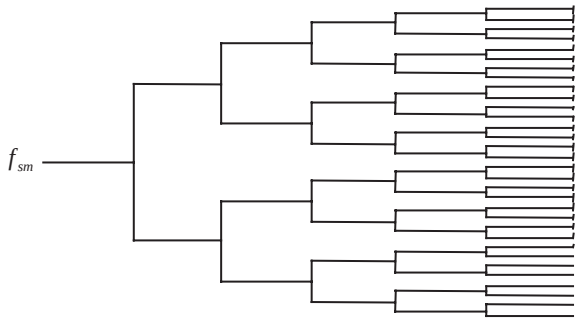

Fig. 6. Layer-to-layer decomposing algorithm of the wavelet-packet.

After this decomposition procedure, the Gray code based sorting [14] must be done to get the function of GC^{-1}, to get an orderly frequency-divided serial. Its deductive expression is as follows (Fig. 6):

$$\begin{aligned}
&GC^{-1}(0) = 0, \quad GC^{-1}(1) = 1;\\
&GC^{-1}(2n) = 2GC^{-1}(n), \quad GC^{-1}(n) \text{ be even};\\
&GC^{-1}(2n) = 2GC^{-1}(n) + 1, \quad GC^{-1}(n) \text{ be odd};\\
&GC^{-1}(2n+1) = 2GC^{-1}(n) + 1, \quad GC^{-1}(n) \text{ be even};\\
&GC^{-1}(2n+1) = 2GC^{-1}(n), \quad GC^{-1}(n) \text{ be odd}.
\end{aligned} \tag{22}$$

4.2.2. Fast reconstruction algorithm of the wavelet-packet

Above layer-to-layer decomposition brings well-distributed frequency-bands. In this paper, only several important frequency-bands as discussed will be interested in. A fast reconstruction algorithm can be arranged as follows:

(1) Choosing the suitable orthogonal conjugate filters H and G.
(2) Selecting the decomposing layers J and routes (Fig. 7). If the length of original signal $u(t)$ equals 2^N, its sampling frequency is f_{sm} and we are only interested in the m frequency-bands at the jth layer, we can get it as $\{n_1, n_2, \ldots, n_m\}$.
(3) Decomposing $u(t)$ by using Eq. (22), a new serial can be obtained as follows:

$$nC_{i,J}(t) = C_{i,J}(t), \quad i = \{n_1, n_2, \ldots, n_m\}; \qquad nC_{i,J}(t) = 0, \quad i \neq \{n_1, n_2, \ldots, n_m\}. \tag{23}$$

(4) Reconstructing the original signal with interested frequency components:

$$C_{i,j}(t) = 2[H^* C_{2i-1,j+1}(t) + G^* C_{2i,j+1}(t)]. \tag{24}$$

A simulating signal $u(t) = \sin(2\pi f_1 t) + \sin(2\pi f_2 t) + n(t)$ is designed to verify the above algorithm (Fig. 8). $f_1 = 700$ Hz, $f_2 = 60$ Hz and $n(t)$ is Gaussian noise. Obviously, the fast wavelet-packet reconstruction algorithm can perfectly extract the interested frequency components from a complex signal with much less power-leaking and aliasing effects than the commonly used FIR filters.

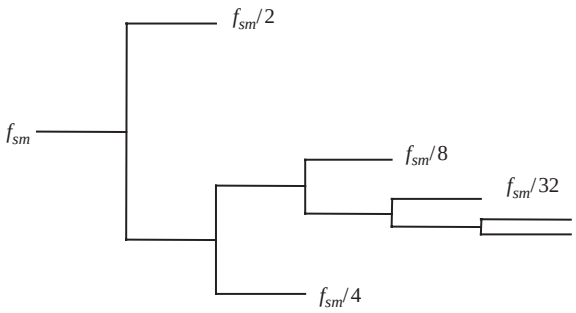

Fig. 7. Fast reconstruction of the wavelet packet.

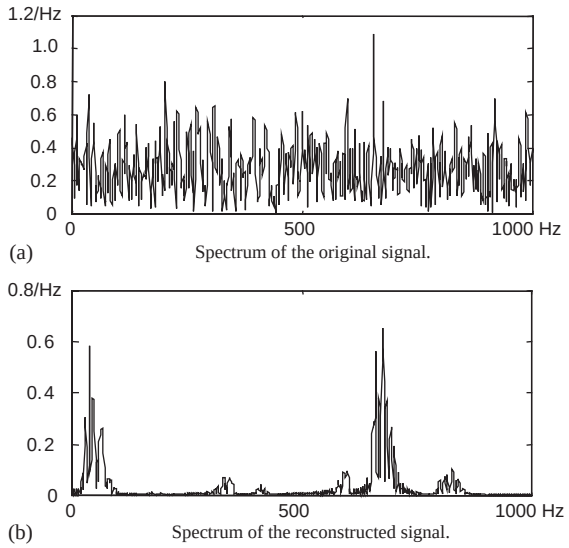

Fig. 8. Simulation of the fast wavelet packet reconstruction algorithm.

Directed by the discussion of Eq. (4), signature extraction of the inner-cylinder excitations is performed by using the above designed wavelet packet based multi-band optimal filtering technique. Fig. 9(a) shows the extracted high-frequency combustion component of the 6190Z_LC diesel engine inner-cylinder excitation while Fig. 9(b) shows the low-frequency compressive one. Obviously, this result coincides with the theoretical discussion from Eqs. (1)–(4).

4.3. Time-frequency signature extraction

As derived in Eqs. (17) and (18), the time-frequency expression based on the non-stationary correlation definition can more reasonably describe the time-varying property and composition of the time-varying engine vibration. Based upon this understanding, a new time-frequency signature

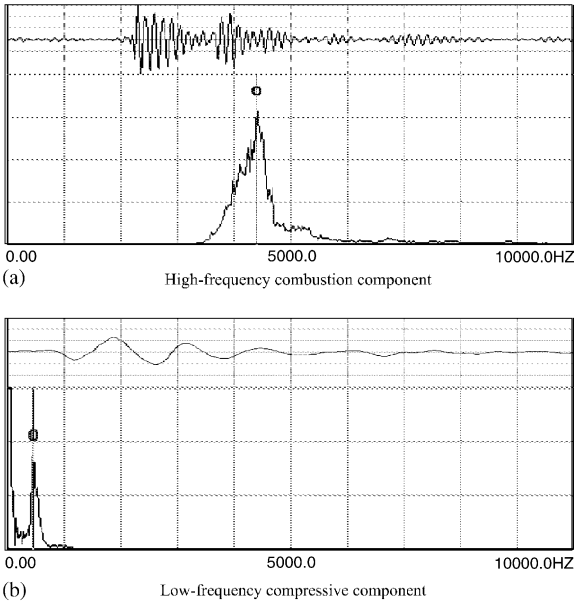

Fig. 9. Signature extraction of the inner-cylinder excitation.

extracting method named as the auto-regressive model based pseudo Wigner-Ville distribution (AR-PWVD) is designed and applied into this research work [13].

4.3.1. Definition of the PWVD

According to the traditional definition of Wigner-Ville Distribution (WVD) made by Clessen in 1980 [11], its continuous expression is the same as shown in Eq. (17). However, in practical application, the continuous vibration signal $u(t)$ is treated as a discrete time series $u(n)$ $(n = 1, 2, \ldots, N)$. In this case Eq. (17) (PWVD-pseudo-WVD) is expressed as

$$W_u^C(n,\omega) = 2\sum_{k'=2}^{2N} u\left(n + \frac{k'}{2}\right) u^*\left(n - \frac{k'}{2}\right) \mathrm{e}^{-\mathrm{j}k'\omega}, \quad k' = 2, 4, \ldots, 2N. \tag{25.1}$$

Letting $k' = 2k$, then

$$W_u^C(n,\omega) = 2\sum_{k=1}^{N} u(n+k)\, u^*(n-k)\mathrm{e}^{-2\mathrm{j}k\omega}. \tag{25.2}$$

Its frequency-domain sum can therefore be derived as

$$\sum_{n=1}^{N} W_u^C(n,\omega) = |S_u(\omega)|^2 + |S_u(\omega+\pi)|^2. \tag{25.3}$$

In a theoretical sense, Eq. (25) demonstrates its suitability in describing the time-varying engine vibration. However, in practical application, it is clearly seen that there are some fatal disadvantages existing in this discrete algorithm, which seriously impede its effective application. These

include: (1) the aliasing phenomenon along its frequency axis as shown in Eq. (25.3); (2) its low frequency-resolution ($\Delta f_{WVD} = 1/2N\Delta t < \Delta f_{FFT} = 1/N\Delta t$) unsuitable for the impact response description as shown in Eq. (25.1) and, (3) its huge data size $2N \times 2N$ unsuitable for signature extraction as shown in Eq. (25.1).

4.3.2. Design and application of the AR-PWVD

In order to overcome the above disadvantages of the PWVD, a more reasonable definition $W_u^P(n,\omega)$ made by Peyrin in 1986 is introduced into the original expression (25.1) [12].

Substituting $n + k'/2 = k, n - k'/2 = n' - k$ into Eq. (25.1), then

$$W_u^P(n',\omega) = 2\sum_{k=1}^{N} u(k)\,u^*(n'-k)\mathrm{e}^{-2\mathrm{j}\omega(2k-n')}. \tag{26.1}$$

Letting $n' = 2n,\ n = 1,2,\ldots,N$, then

$$W_u^P(2n,\omega) = 2\sum_{k=1}^{N} u(n+k)\,u^*(n-k)\mathrm{e}^{-2\mathrm{j}\omega(2k)} = \frac{1}{2}\,W_u^C(n,\omega). \tag{26.2}$$

In this case, its frequency-domain sum is

$$\sum_{n=1}^{N} W_u^P(n,\omega) = |S_u(\omega)|^2. \tag{26.3}$$

Comparing Eq. (26.3) with Eq. (25.3), it can be seen that the aliasing phenomenon is overcome in the sense of its frequency-domain sum. Complemented with an analytic transform to the time-varying variable $r_u(n,k) = u(k)\,u^*(n-k)$ in Eq. (25.1), this disadvantage of the PWVD is reduced to its minimum [12,13].

Further taking the analytic transform of the time-varying variable $r_u(n,k)$ as $r_{ua}(n,k)$, then it can be described by using a M order, complex, time-varying auto-regressive time series model ($AR(n,M)$ model) as follows [13]:

$$r_{ua}(n,k) = \sum_{i=1}^{M} \varphi_r(n,i)\,r_{ua}(n,k-i) + a_r(n). \tag{27}$$

Introducing Eq. (27) into Eq. (25.1), an $AR(n,M)$ model based pseudo-Wigner-Ville distribution (AR-PWVD) can be derived as

$$W_u^{AR}(n,f) = 2\mathrm{Re}\left[\sum_{k=1}^{N} r_{ua}(n,k)\mathrm{e}^{-\mathrm{j}2\pi f(2k-n)}\right]. \tag{28.1}$$

It can also be expressed as a form of the time-varying model spectrum

$$W_u^{AR}(n,f) = \frac{\sigma_{ar}^2(n)}{\left|1 - \sum_{i=1}^{M} \varphi_r(n,i)\mathrm{e}^{-2\mathrm{j}\pi f(2i-n)}\right|^2} \tag{28.2}$$

The AR-PWVD shown in Eq. (28) overcomes most the disadvantages of the traditional PWVD. Firstly, its frequency-domain aliasing is reduced to a minimum in this algorithm. Secondly, its time-frequency expression is purely dependent on the auto-regressive model $AR(n,M)$, which

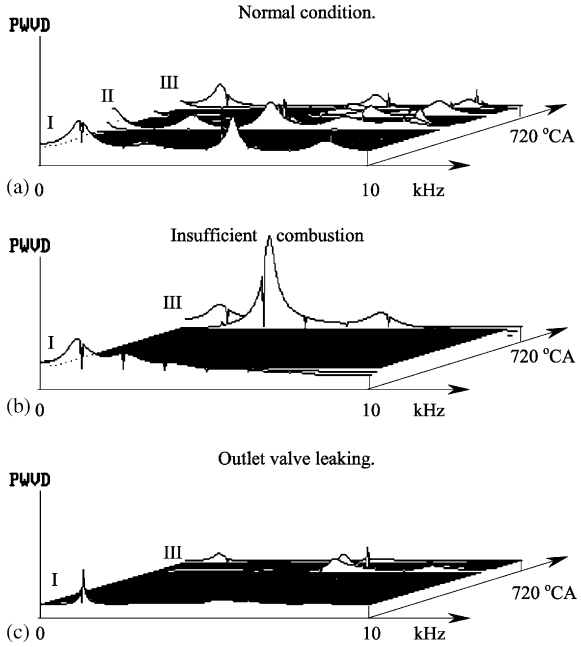

Fig. 10. AR-PWVD of the engine vibration (measured on cylinder cap of the 6190Z_LC diesel engine).

possesses a high frequency resolution to suitably describe the impact response of the engine vibration. The most important advantage of this algorithm over others is probably that all its analyzing messages are concentrated inside the limited model coefficients $\varphi_r(n,i)$ $(i=1,2,\ldots,M$. In this paper, M is less than 10) and residual error $\sigma_{ar}^2(n)$, which is essential for data compression and signature extraction.

Detailed discussions on the AR-PWVD algorithm have been published in Ref. [13]. Practical diagnosing results for three typical working condition (normal, insufficient combustion and outlet valve leaking) of the 6190Z_LC diesel engine are shown in Fig. 10. As a result of the synchronizing filtering pre-treatment as mentioned in Section 4.1, the time axis becomes the engine's crankshaft rotating angle, so that the AR-model spectral frequency compositions as well as the angular positions of the impacting response sections I, II and III as mentioned in Fig. 1 are clearly identified and distinguished between each other. For the normal combustion condition shown in Fig. 10(a), the impacting section I (mainly caused by the inner-cylinder gas excitation), II (mainly caused by the outlet valve impacting) and III (mainly caused by the inlet valve impacting), respectively, shares a reasonable proportions in the AR-PWVD. For the insufficient combustion condition shown in Fig. 10(b), the impacting response mainly caused by the high-frequency inner-cylinder combustion (section I) as well as the outlet valve impacting response (section II) almost disappears from the AR-PWVD. This is a reasonable explanation to the diesel engine's practical working condition. Another reasonable explanation can also be reached from Fig. 10(c) for the corresponding engine working condition. All this means, the AR-PWVD indeed provides a suitably precise time-frequency description of the time-varying engine vibration.

4.3.3. AR-PWVD based signature extraction

By composing the coefficients $\varphi_r(n,i)$ and residual error $\sigma_{ar}^2(n)$ $(i=1,2,\ldots,M)$ of the $AR(n,M)$ model into a message mode vector $\Phi(n)=[\varphi_r(n,1),\varphi_r(n,2),\ldots,\varphi_r(n,m),\sigma_{ar}^2(n)]^T$, the message-distance-based intelligent classification and signature extraction can be performed to it [1,2]. Taking the commonly used J-divergence distance between the reference mode R and the testing mode T of the engine conditions [1,2,4] as an application example, it can be expressed as follows:

$$J(P_R,P_T) = I(P_R,P_T)+I(P_T,P_R) = \frac{1}{M+N+1}\sum_{n=1}^{N} \times \sum_{i=1}^{M+1} \left\{ \begin{array}{l} \dfrac{1}{2\sigma_R^2(n,i)}\left\{\sigma_T^2(n,i)+[\Phi_R(n,i)-\Phi_T(n,i)]^T\gamma_R(n,i)[\Phi_R(n,i)-\Phi_T(n,i)]\right\}+ \\ \dfrac{1}{2\sigma_T^2(n,i)}\left\{\sigma_R^2(n,i)+[\Phi_R(n,i)-\Phi_T(n,i)]^T\gamma_T(n,i)[\Phi_T(n,i)-\Phi_R(n,i)]\right\}-1 \end{array} \right\}. \tag{29}$$

During the experimentation, 6 standard reference fault modes (modes 1–6) are set along with 2 test fault modes (modes 7 and 8) of the 6190Z_LC diesel engine (as laid out in Table 1). The relevant J-divergence distance results based on the AR-PWVD coefficients are listed in Table 2. Classifications in Table 2 (the underlined) clearly indicate that the test modes 7 and 8, respectively,

Table 1
Simulated fault modes of the 6190Z_LC diesel engine (1500 rev/min)

Mode	1	2	3	4	5	6	7	8
Inlet valve Clearance (mm)	0.43 (normal)	0.23 (max)	0.63 (min)	Spring Breaking	0.43 (normal)	0.43 (normal)	0.43 (normal)	0.43 (normal)
Outlet valve Clearance (mm)	0.48 (normal)	0.28 (max)	0.68 (min)	0.48 (normal)	Spring breaking	Leaking	0.28 (max)	0.68 (min)

Table 2
J-divergence distance results based on the AR-PWVD

Mode	1	2	3	4	5	6	7	8
1	0.00	3.51	3.79	6.96	3.11	3.72	4.41	11.42
2	3.51	0.00	2.62	3.86	2.20	6.10	**1.31**	7.92
3	3.79	2.62	0.00	4.26	5.32	6.34	7.27	**1.06**
4	6.96	3.86	4.26	0.00	8.38	14.22	8.68	13.55
5	3.11	2.20	5.32	8.38	0.00	2.82	3.42	2.02
6	3.72	6.10	6.34	14.22	2.82	0.00	8.91	1.70
7	4.41	**1.31**	7.27	8.68	3.42	8.91	0.00	2.77
8	11.42	7.92	**1.06**	13.55	2.02	1.70	2.77	0.00

approach the reference modes 2 and 3, which coincide with the fault mechanism and changing tendency of the engine. This also explains the suitability of AR-PWVVD to an integrated signature extraction of the engine vibration.

5. Conclusions

As a stage summary of the authors' serial researches on the reciprocating engine vibration and condition monitoring [3,4,13], this paper presents a systemic and detailed discussion successively on the impacting excitations, time-varying vibration characteristics and applicable analyzing and diagnosing strategy of the reciprocating engine. Through in-depth theoretic derivations respectively on the time-domain, high-order-frequency-domain and time-frequency-domain characteristics of the engine vibration, reasonable description and applicable methodologies for the engine vibration analysis and condition monitoring are concluded. Satisfactory verification is also carried out via suitable designed experimentation. The significance of this paper lies in the following aspects:

(1) A detailed investigation is made to the widespread inner-engine impact excitations.
Theoretical derivation is made to the engine inner-cylinder working process. Oscillating performance of the inner-cylinder gas excitation is theoretically analyzed and the high-frequency mechanical and fluid impacts are reasonably classified. This work lays down an important foundation for the further investigation into the engine vibration characteristics and design of the suitable diagnostic strategies.
(2) A detailed theoretical analysis is made to the time-varying engine vibration response.
Based upon the above investigation on the inner-engine impacting excitations, a theoretical model is developed to describe the time-varying engine vibration response. Derivation of the time-domain, high-order frequency-domain and time–frequency-domain interdependent relations of the impacting excitations and the engine vibration, from a strict theoretic viewpoint, supplies a reasonable description and applicable methodologies for the engine vibration analysis and condition monitoring.
(3) Applicable vibration analyzing and condition monitoring strategies for the diesel engine are designed and applied into the practical engineering.

Following the theoretical research conclusions gained in this paper, practical analyzing and diagnosing methods are designed and applied to the $6190Z_LC$ diesel engine. These include the software-based instantaneous synchronizing filtration for the pre-treatment of the time-varying engine vibration signal; the wavelet-packet based multi-band optimal filtering technique for signature extraction of the inner-cylinder impact excitations; as well as the AR-PWVD time-frequency analysis method for an integrated signature extraction of the engine vibration. Finally, experiments on the $6190Z_LC$ diesel engine verified the validity and practicability of these methods in practical engineering.

Acknowledgements

This work was sponsored by the NSFC (Approved No.: 59775024) and the K.C. Wong Education Foundation in Hong Kong.

References

[1] Cempel C. Vibroacoustic condition mornitoring. London: Ellis Horwood Ltd.; 1994.
[2] Lyon RH. Machinery noise and diagnostics. New York: Butterworths; 1987.
[3] Geng ZM. Research on the vibroacoustic features and diagnosing approaches of the diesel engine. Transactions of CSICE 1995;13(2):11–25.
[4] Geng ZM. Some techniques applicable to the non-stationary vibration analysis and fault diagnosis of the reciprocating machinery. Chinese Journal of Mechanical Engineering 1996;32(4):110–21.
[5] Gu F, Jacob PJ, Ball AD. Non-parametric models in the monitoring of engine performance and condition—Part 2: Non-intrusive estimation of diesel engine cylinder pressure and its use in fault detection. ImechE. Proceedings Part D, Journal of Automobile Engineering 1999;213:135–43.
[6] Jones NB. A review on condition monitoring and fault diagnosis for diesel engines. Condition monitoring'97. Xi'an, P. R. China: National defense industry press; 1997. p. 221–42.
[7] Jeung Kim T, Lyon RH. Cepstral analysis as a tool for robust processing. Journal of Mechanical System and Signal Processing 1992;6(1):1–15.
[8] Cartmell M. Introduction to linear, parametric, and non-linear vibrations. London: Chapman & Hall; 1990.
[9] Lonmann AW. Triple correlation. IEEE 1984;72(7):1042–53.
[10] Lii KS. Cross-bispectrum computation and variance estimation. ACM Transactions on Mathematical Software 1981;7(1):66–87.
[11] Classen TA. The Wigner distribution—a tool for time-frequency signal analysis. Philips Journal of Research 1980;35.
[12] Peyrin FA. A unified definition for the discrete-time, discrete-frequency, and discrete-time/frequency Wigner distributions. IEEE Transactions On ASSP, 1986, pp. 858–68.
[13] Geng ZM. Some modifications on the Wigner distribution for application into the non-stationary vibration analysis and fault diagnosis. Journal of Signal Processing 1995;11(2):116–23.
[14] Aguirre J. Basis of wavelets and atomic decompositions of $H^1 \to (R^n)$ and $H^1 \to (R^n \times R^n)$. Proceedings of AMS 1991;111(3):683–93.
[15] Rioul O, Duhamel P. Fast algorithm for discrete and continuous wavelet transforms. IEEE Transactions on Information Theory 1992;38:569–86.